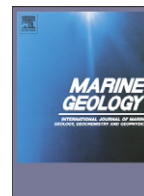




Contents lists available at ScienceDirect

Marine Geology

journal homepage: www.elsevier.com/locate/margeo

Tide-driven dune migration and sediment transport on an intertidal shoal in a shallow estuary in Devon, UK

Gerd Masselink*, Laurie Cointre, Jon Williams, Roland Gehrels, Will Blake

School of Geography, University of Plymouth, United Kingdom

ARTICLE INFO

Article history:

Received 12 June 2008

Received in revised form 4 March 2009

Accepted 15 March 2009

Available online xxxx

Communicated by John T. Wells

Keywords:

Intertidal dunes

Bedforms

Bedload equations

Sediment transport

Estuarine evolution

ABSTRACT

The migration of subaqueous dunes was investigated over a 3-month period on an intertidal shoal near the mouth of the shallow mixed wave/tide dominated Avon Estuary on the Channel coast of southwest Britain. The dunes, characterised by heights and lengths of 0.05–0.2 m and 5–10 m, respectively, migrated 10–20 m over the 3-month period, representing an average volumetric sediment transport rate of 0.5 m³ per unit meter width. Compared to equilibrium models of dune dimensions based on the water depth, the dune height was predicted well, but the dune length was under-predicted. Sediment transport on the intertidal shoal was controlled by a distinct tidal asymmetry, with maximum flow velocities during flood (0.4–0.5 m s⁻¹) significantly stronger than during ebb (0.2–0.3 m s⁻¹). Predicted bedload transport based on theory underestimates the actual transport and this is attributed to the modest flow velocities encountered and, perhaps, the importance of suspended load transport. However, when empirically calibrated and related to tide range, the transport equation adequately accounts for observed rates. Using nearby tidal observations, the predicted annual volumetric sediment transport rate is 2.6 m³ per unit meter width. This estimate compares favourably with the annual volumetric sediment transport based on dune measurements (2.0 m³). Using the notion that the transport rate decreases on the intertidal shoal in the up-estuary direction to zero at its up-estuary end, a vertical accretion of 0.5 cm yr⁻¹ was predicted. The main implication of our study is that accurate and well-designed process measurements of dune dynamics and tidal currents can provide useful information on the longer term evolution of intertidal shoals in sandy, shallow (flood-dominant) estuaries.

© 2009 Elsevier B.V. All rights reserved.

1. Introduction

Subaqueous dunes are common features in estuarine environments and develop in fine-to-medium sand-sized sediments when flow velocities are 0.5–1 m s⁻¹ (Ashley, 1990). They are of major importance in controlling estuarine sediment dynamics either indirectly, by presenting important bed roughness elements that retard tidal flows, or directly, because their migration constitutes net sediment transport. Past studies of tidal dune dynamics have mainly focussed on identifying transport regimes and depth-scaling rules (e.g. Terwindt and Brouwer, 1986; Larcombe and Ridd, 1995; Kostaschuk and Villard, 1996; Larcombe and Jago, 1996; Cheng et al., 2004; Francken et al., 2004; Villard and Church, 2005; Bartholdy et al., 2005) or on exploring the relationship between measured rates of dune migration and predicted bedload transport rates (e.g. Hoekstra et al., 2004; Kostaschuk and Best, 2005; Williams et al., 2006). Considering the difficulty in determining net sediment transport in estuarine environments, surprisingly few investigations have utilised measurements of dune dynamics over extended periods of time to gain insight in net sediment transport patterns and ensuing implica-

tions for morphological development (Shepard and Hails, 1984; Allen et al., 1994; Gonzalez and Eberli, 1997; Whitmeyer and FitzGerald, 2008). It is, however, acknowledged that repeated, high-accuracy measurements of sedimentary bedforms has significant implications for long-term modelling of estuarine sediment transport (Bates and Oakley, 2004).

This paper uses field surveys of a dune field over a 3-month period complemented by measurements of tidal flows and water levels to gain insight into the net sediment transport rates and morphological development of an intertidal shoal in a small and shallow wave/tide-dominated estuary. Measured dune migration rates were converted to sediment transport rates and compared with volumetric transport predicted by empirical formulae. Because the dunes are only affected by flood currents, an expression of net transport rate as a function of the ocean tide range could be derived. Using tidal predictions, this expression was then used to estimate the annual net sediment transport over the shoal and the resulting morphological development.

2. Study area

The Avon estuary is located on the south coast of Devon in southwest England (Fig. 1). It is a relatively small estuary with a total surface area of 213.5 ha, of which 146.2 ha are intertidal, an estuarine

* Corresponding author.

E-mail address: gerd.masselink@plymouth.ac.uk (G. Masselink).

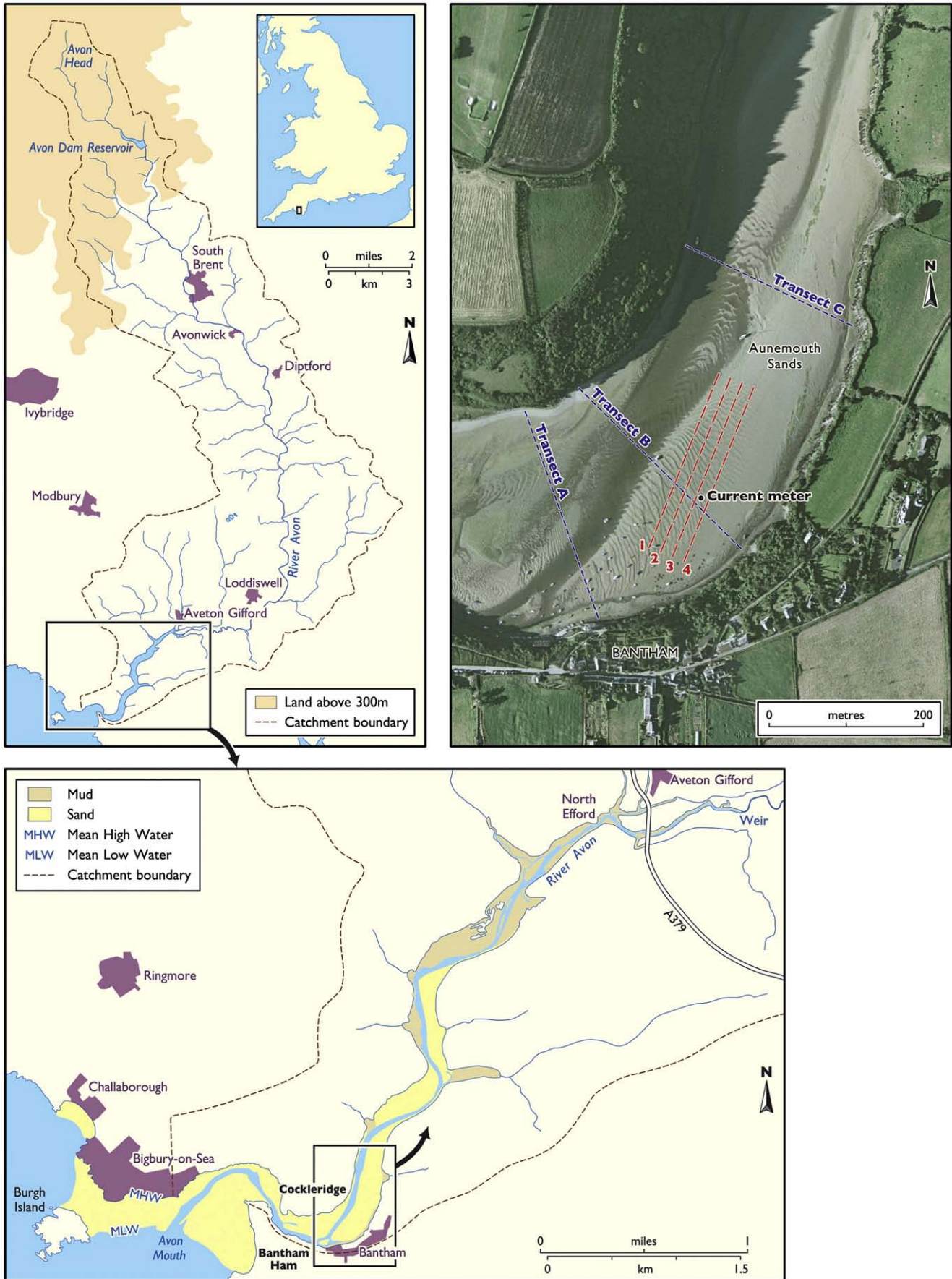


Fig. 1. Location map of the Avon estuary and aerial photograph of Aunemouth Sands showing the dune field, locations of cross-channel transects A–C, survey lines 1–4 and position of the current meter (photo from GoogleEarth).

shoreline length of 19.8 km and a 7.8-km long tidal channel (Davidson, 1991). The estuary has steep-sided margins, cut into relatively weak Devonian slates and grits, and is generally considered a *ria*-type (drowned river) estuary. However, the Avon estuary could equally be termed a *bar-build* estuary, because it has two sand barriers at its mouth: Bantham Ham and Cockleridge. It should be pointed out, however, that Bantham Ham is not entirely depositional, but represents a raised interglacial shore platform capped with coastal dunes, fronted by a relatively thin beach deposit.

The five main depositional environments in the Avon estuary include beach and dune deposits at Bantham Ham and Cockleridge, an extensive ebb-tidal delta forming part of the tombolo behind Burgh Island, a flood tidal delta with several intertidal shoals in the outer estuary, a main tidal channel that meanders along the entire estuary with a tidal weir at Aveton Gifford and salt marshes in the upper estuary (Fig. 1). The estuary thus displays both wave-dominated (beach, dunes, tidal deltas) and tide-dominated features (meandering tidal channel, salt marshes), and is perhaps best classified as a mixed wave-tide dominated delta (Dalrymple et al., 1992). The tidal channel has a scoured appearance over most of the lower and upper estuary. The estuary is relatively pristine and the only human modifications comprise several wooden groins at Cockleridge (built in the 1930s and now largely obsolete) and the reclamation of a 15-ha salt marsh in the upper estuary more than 100 years ago.

The mixed wave-tide character of the estuary is explained by the wave and tidal forcing. Offshore waves are prevailing from the SW quadrant (mainly swell), but also from the SE quadrant (mainly sea), and are fairly energetic. Offshore waves exceed 1.5 m for 10% of the year and 0.5 m for 75% of the year (Draper, 1991), but the inshore waves are expected to be significantly less due to refraction. The protection provided by Burgh Island from SW waves is considerable (Fig. 1) and it is likely that the most energetic inshore wave conditions affecting the mouth of the Avon estuary are from the SE quadrant. Ocean tides at the Avon estuary are slightly less than at Devonport (Plymouth; closest Primary Port for tidal data) and are characterised by a mean spring and neap tide range of 4.3 and 2.0 m, respectively (Uncles et al., 2007). The elevation of the high water levels during spring and neap tides at the mouth of the estuary are estimated at 2.5 and 1.2 m ODN (Ordnance Datum Newlyn, which is the mean sea level datum in the UK), respectively. The 1:50 year storm surge height along the south coast of Devon is c. 0.5 m (Lowe and Gregory, 2005); therefore, observed water levels correspond generally well with tidal predictions.

The tide range at the mouth in combination with the morphology of the tidal channel can be used to determine whether an estuary is ebb- or flood-dominant using the model of Friedrichs and Aubrey (1988). According to this model, estuaries can be classified on the basis of the ratio between the amplitude of the M2 tidal constituent and the average depth of the tidal channel at mid-tide. When this ratio is larger than 0.4, the estuary is shallow and flood-dominant; when the ratio is smaller than 0.3, the estuary is deep and ebb-dominant. At the mouth of the estuary, the amplitude of the M2 tidal constituent is 1.5 m (Admiralty Tide Tables, 2007) and the mean channel depth at mid-tide is 2 m (Uncles et al., 2007). The resulting ratio is 0.75, suggesting that the estuary is shallow and flood-dominant, and the mouth should be a net importer of marine sediments.

Freshwater discharge into the Avon estuary is mainly through the Avon River supplemented with minor contributions from small streams draining the valley slopes. River discharge is measured by an automatic gauging station at Loddiswell located c. 3 km upstream from the tidal limit (Fig. 1). A pronounced seasonal cycle in river discharge is apparent with a monthly-averaged winter discharge of just under 7 cumecs ($\text{m}^3 \text{s}^{-1}$) and a monthly-averaged summer discharge of just over $1 \text{ m}^3 \text{ s}^{-1}$ (Uncles et al., 2007). Peak flows during winter occasionally exceed $40 \text{ m}^3 \text{ s}^{-1}$ and minimum flows in summer are often less than $0.5 \text{ m}^3 \text{ s}^{-1}$.

The only investigation into tidal hydrodynamics in the Avon estuary has been carried out by Uncles et al. (2007), who deployed current meters in the tidal channel at Bantham Harbour (lower estuary) and north Efford (upper estuary) over 1-week periods during summer and winter in 2006. At Bantham Harbour, during both summer and winter, peak flows during flood ($0.4\text{--}0.8 \text{ m s}^{-1}$) were weaker than during ebb ($0.6\text{--}1 \text{ m s}^{-1}$) and the salinity profile was well-mixed. At north Efford, during summer, peak flood flows ($0.5\text{--}0.6 \text{ m s}^{-1}$) were stronger than during ebb ($0.3\text{--}0.4 \text{ m s}^{-1}$) and the salinity profile was well-mixed during flood, but stratified during ebb. During winter, however, flows in the upper estuary were almost exclusively directed seaward with peak velocities of $0.4\text{--}0.7 \text{ m s}^{-1}$. Significant damping of the tidal wave occurs into the estuary and for a typical ocean tide range of 3.7 m the tide range at Bantham Harbour and north Efford was 3.0 and 1.5 m, respectively. In addition, distortion of the tidal wave was also evident with a duration of the flood phase at Bantham Harbour of only 4–5 h. The role of locally-generated wind waves was found to be very limited with significant wave heights less than 0.1 m at in the lower estuary and less than 0.05 m in the upper estuary. Uncles et al. (2007) also conducted 1-line modelling of the tidal motion in the Avon estuary and computed that the tidal prism up-estuary from Bantham Harbour was $1.7 \times 10^6 \text{ m}^3$ during spring tide and $0.7 \times 10^6 \text{ m}^3$ during neap tide (Uncles, pers. comm.).

This investigation focuses on an extensive field of medium, 2-dimensional subaqueous dunes (defined following Ashley (1990) using the length of the bedform as the classifier) found on Aunemouth Sands, an intertidal shoal located just up-estuary from Bantham Harbour east of the main tidal channel (Fig. 1). The shoal is roughly 600 m long and 100 m wide, and is tapered at its down-estuary end and merges with a featureless sand flat at its up-estuary end. The shoal is separated from the eastern bank by a small drainage channel that originates at the north-eastern end of the shoal and joins the main tidal channel at the south-western end. Map analysis reveals that this channel was considerably more important in 1954 than at present (Millin, 2006), suggesting it is progressively filling in. This is also suggested by the prevailing muddy sediments present in this channel.

3. Methods

3.1. Estuarine morphology

An extensive survey of the Avon estuary was carried out in 2005 by WS Atkins Consulting using dGPS and commissioned by the Aune Conservation Association (<http://www.aca.aveton-gifford.co.uk/>; unpublished data). Over 14,000 survey points were collected more or less uniformly from the entire estuary, except the ebb tidal delta, and ARC-GIS was used to extract cross-channel transects at c. 30-m intervals. These data were used to determine the variation along the estuary in tidal channel depth, channel width and cross-sectional area, and also to obtain information on the elevation of the intertidal shoals and the salt marsh surface.

3.2. Dune morphology, migration and sediment transport rates

The dunes at Aunemouth Sands were surveyed every two weeks from 13/07 to 12/10 (in 2007) along four lines (Fig. 1). An additional survey was carried out on 10/02/08 following an extended period of high river discharge to verify that the dune field persists through the winter season. The survey lines were 240 m long and spaced at 16 m with their heading representing a compromise between the length axis of the shoal and the orientation of the dunes. Line 1 skirted the edge of the main tidal channel and Line 4 ran more or less along the central axis of the shoal. Surveys were conducted with a laser total station which has a vertical and horizontal accuracy of $O(\text{mm})$ and $O(\text{cm})$, respectively. Care was taken during the surveys to stay within 0.2 m of the line and measurements were taken about every

meter or closer in case of steep morphological gradients (e.g. crest of the dune).

The heading of the survey transects is generally not perpendicular to the orientation of the dune crests (Fig. 1) and not accounting for this difference would result in an overestimation of the dune length and migration rate. The orientation of the dunes varies in space (across and along the shoal) and time (during the survey), but is generally between 0° and 45° (refer to Fig. 1). The dune crest lines were mapped just prior to the first survey on 13/07/2007 (Cointre, 2008) and indicate an average 'misalignment' of the survey grid of 30° . The dune lengths and migration rates (and hence the derived sediment transport rates) were therefore reduced by a factor 0.87 (cosine of 30°). For a misalignment error of 0° and 45° the correction factor should be 1 and 0.71, respectively, which is within 20% of the used correction factor.

The survey period encompassed 6 spring-to-spring tidal cycles and the maximum and minimum tide range experienced, as predicted for Devonport, was 5.5 and 1.6 m, respectively (Fig. 2). Despite the survey being carried out during summer/autumn, the freshwater discharge of the Avon River was always more than $1 \text{ m}^3 \text{ s}^{-1}$ and the daily-averaged discharge exceeded $5 \text{ m}^3 \text{ s}^{-1}$ for a number of days. Maximum freshwater discharge occurred between Surveys 4 and 5.

The survey lines were linearly interpolated at 0.25-m intervals and, rather than conducting a wave-by-wave analysis, the data were subjected to time series analysis techniques using a 50-m moving window. A number of dune properties were computed over these 50-m data windows. Dune height η was estimated by multiplying the standard deviation of the detrended bed-level time series by 4 and dune length λ was determined from the peak in the spectrum of the bed-level time series (Austin et al., 2007). The vertical asymmetry of the dunes, i.e., whether they are flood- or ebb-directed, was

determined by first taking the first derivative of the bed-level time series $a = dz/dx$ and then computing the normalised skewness of a through $A = -(a^3/a^2)$. This method is similar to that used by Hoefel and Elgar (2003) to quantify the shape of ocean waves. $A=0$ represents symmetrical dunes; $A>0$ represents flood-directed dunes; and $A<0$ represents ebb-directed dunes.

The migration distance over the different survey intervals was determined by carrying out a cross-correlation between successive survey lines and identifying the lag associated with the maximum cross-correlation (Larcombe and Jago, 1996). Aliasing could be a potential problem with this methodology, but daily dune observations conducted prior to the main survey (Cointre, 2008) indicated that the maximum migration distance over a spring-to-spring tidal cycle is always less than one dune wave length. Cross-correlation coefficients were generally larger than 0.75 and always larger than 0.5, ensuring that the lags correctly indicate migration distances. The migration distance was converted to migration rate per tide V_{mig} by taking into account the number of tides between successive surveys. The dune migration rates were converted to a volumetric transport rate q_d according to

$$q_d = a_m \eta V_{\text{mig}} \quad (1)$$

where a_m is a factor accounting for porosity and dune shape. A range of values for a_m (0.2–0.37) are quoted in the literature (cf. van den Berg, 1987; Hoekstra et al., 2004) and in this study $a_m = 0.32$ will be assumed (Soulsby, 1997, p.118). The volumetric sediment transport rate is in $\text{m}^3 \text{ tide}^{-1}$ per meter width ($\text{m}^2 \text{ tide}^{-1}$). In the remainder of this paper we will use the unit m^2 to indicate the volumetric transport per meter width. The sediment transport derived from dune migration is generally considered the bedload component of the total load transport; however, suspended transport may also contribute sig-

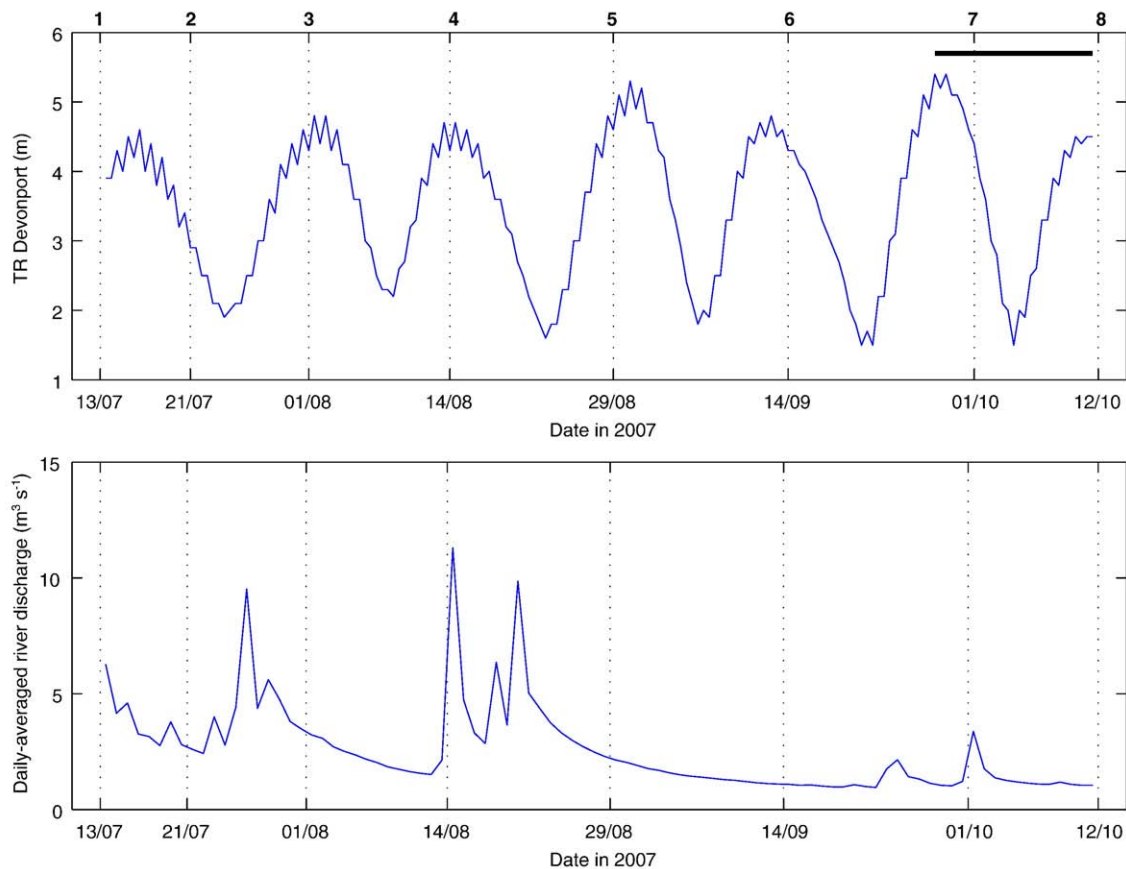


Fig. 2. Timing of the dune surveys in relation to the tide range TR at Devonport (upper panel) and the daily-averaged river discharge recorded at Loddiswell (lower panel). The thick horizontal line in the upper panel indicates the timing of the hydrodynamic measurements, and the numbers and dashed lines refer to the dune surveys.

nificantly to dune migration (e.g., Kostaschuk and Best, 2005). Therefore, although it is possible, if not likely, that bedload is the main transport mode responsible for dune migration, the transport rate derived from the latter cannot automatically be considered the bedload component of the total transport. Because the analysis of the dune geometry and migration rate is conducted using a moving window, the variation in the sediment transport rate along the survey lines is obtained. This enables investigating the spatial gradients in the sediment transport rate which is useful for assessing the morphological development of the shoal due to dune migration.

3.3. Current velocities, water levels and predicted sediment transport rates

A Valeport electromagnetic current meter with a Druck pressure transducer was deployed in the middle of the intertidal shoal from 28/09 to 12/10 (in 2007) and recorded flow velocities and water levels over 27 tidal cycles over a spring-to-spring tidal cycle. The instruments were installed on Line 3 at $x = 86$ m from the start of the survey line (Fig. 1). Current velocities and water levels were recorded at 4 Hz and 1 Hz, respectively, and data were block-averaged every 10 min. Flow velocities were recorded at c. 0.25 m above the bed; hence, flows in very shallow water were not recorded. The current meter was deployed just up-slope from the dune crest, and its distance from the bed is only expected to have varied by a few centimetres during the experiment due to the gentle back-slope of the dune (<0.02) and the limited dune migration during the deployment period (c. 2 m). The dune was asymmetric and pointed up-estuary, and its height and length were 0.15 and 8 m, respectively. Migration rates of the dune over which the flow velocities were recorded were monitored using stakes inserted at the base of the slip-face over an area of 25 m at either side of the instrument location. Measurements of the position of the stakes were made over 5 time intervals: 28/09–29/09

(Tides 1–2), 29/09–01/10 (Tides 3–6), 01/10–05/10 (Tides 7–13), 05/10–08/10 (Tides 14–19) and 08/10–12/10 (Tides 20–27). Data from the different stakes were averaged to obtain mean and representative dune migration distances and rates.

The velocity measurements were used to predict the bedload sediment transport rate using the following procedure (see Soulsby, 1997; pp. 46–48 and 158–160). An approximation to the skin friction bed shear velocity u_* produced by and acting on sediment grains was computed from the velocity data under the assumptions that the bed was hydrodynamically rough and the velocity profile conformed to a logarithmic law in the form of

$$u_* = \frac{\kappa u_z}{\ln(z/z_0)} \quad (2)$$

where κ is von Karman's constant ($\kappa=0.4$), u_z is velocity measured at height z from the bed ($z=0.25$ m) and z_0 is bed roughness length attributable to the sediment grains given by $z_0 = d_{50}/12$, where d_{50} is median sediment size ($d_{50}=0.3$ mm). In support of the first assumption we argue that the 'constant stress' log-layer applies to the portion of the bottom boundary layer where acceleration is much weaker than friction, and where the stress approximates the bed shear stress. For the present tidal boundary layer in the estuary, the ratio of acceleration to friction scales as ω^2/ε , where the tidal radian frequency $\omega \approx 1.4 \times 10^{-4} \text{ s}^{-1}$, z is the elevation above the bed, ε is the eddy viscosity (typically $10^{-3} \text{ m}^2 \text{ s}^{-1}$; Friedrichs and Hamrick, 1996). Thus the log-law used here to estimate bed shear stress should be applicable for $z < \approx \sqrt{(0.1\varepsilon/\omega)} \approx 0.84 \text{ m}$. It is noted also that friction is still $O(10)$ times the magnitude of acceleration at $z < 0.27$ m even when ε is reduced by a factor of 10 supporting further the assumption of a log-law in the flow region $0 < z < 0.5$ m. The

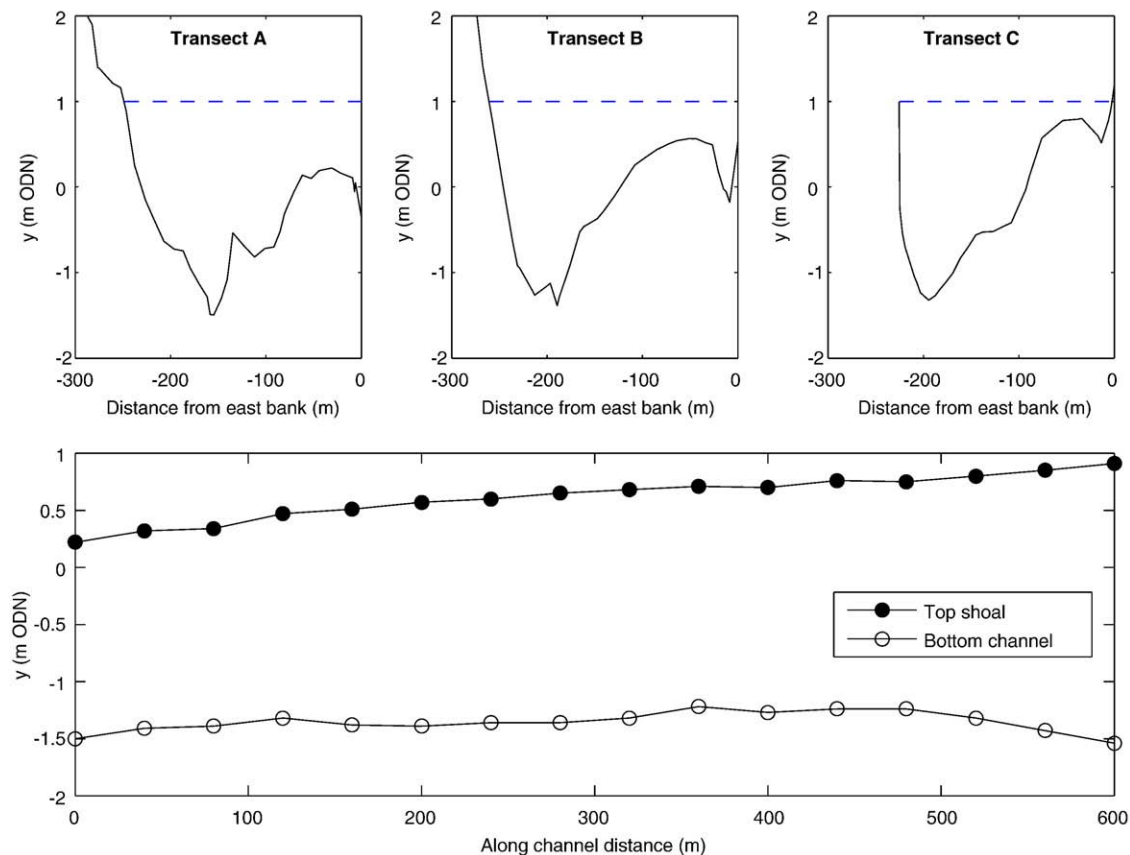


Fig. 3. Upper panels: cross-channel morphology for three transects cutting across the intertidal shoal at Aunemouth Sands and the main tidal channel (see Fig. 1 for transect locations). Lower panel: along-channel variation in the elevation of the top of intertidal shoal and the deepest part of the main tidal channel. The horizontal dashed line in the upper panels represents 1 m ODN, which is approximate neap high tide level.

assumption of hydrodynamically rough flow could be challenged as in most cases flow over sandy sediment is transitional. However, the error in the calculation of u_* resulting from considering the flow to be rough turbulent is less than 10% (Soulsby, 1997; p. 47) and, given the limitations of the other data in this study and the additional complexity of computing skin friction bed shear velocity for transitional flows, this approach is considered to be a good practical compromise. The bed shear stress τ_0 was then obtained from $\tau_0 = \rho u_*^2$ and used to compute the Shields parameter θ

$$\theta = \frac{\tau_0}{g\rho(s-1)d_{50}} \quad (3)$$

where g is gravity ($g = 9.8 \text{ m s}^{-2}$), ρ is water density ($\rho = 1025 \text{ kg m}^{-3}$) and s is ratio of densities of sediment and water ($s = 2.58$). The dimensionless bedload transport rate ϕ was then computed using the Meyer-Peter and Muller (1948) equation (henceforth referred to as the 'MPM equation')

$$\phi = 8(\theta - \theta_t)^{1.5} \quad (4)$$

where θ_t is the value of θ at the threshold of motion ($\theta_t = 0.05$). The dimensionless transport rate ϕ was then converted to a volumetric transport bedload rate q_b using

$$q_b = [g(s-1)d_{50}^3]^{0.5} \phi \quad (5)$$

where q_b is in $\text{m}^2 \text{ s}^{-1}$. By integrating the predicted sediment transport rates over individual tidal cycles they can be directly compared with the measured transport rates obtained from dune migration.

In the present current-only flow regimes, the MPM equation was selected for a number of reasons including simplicity, widespread use, past validation in similar environments to the present and suitability for the present range of grain sizes. For comparison, we have also used three additional formulations: Madsen (1991), Nielsen (1992) and the 'simplified' sediment transport model of van Rijn (1993). These equations are given in Appendix A.

4. Results

4.1. Morphology at Aunemouth Sands

Analysis of surficial sediment samples showed that the sediment size on the shoal is characterised by a median sediment size d_{50} of 0.25–0.35 mm and a d_{90} of 0.4–0.5 mm. The survey data complemented by field observations reveal that the dunes at Aunemouth Sands have heights and lengths of 0.05–0.25 m and 5–15 m, respectively, and are almost all oriented up-estuary. Smaller current ripples with heights of c. 0.03 and lengths of c. 0.15 m are superimposed on the dunes. These ripples are notably three-dimensional with along-ripple lengths scales $O(0.5 \text{ m})$. They are flood-directed, but are often characterised by an ebb-directed 'lip' on the crest. Some of the dunes at the edge of the tidal channel in Line 1 are oriented down-estuary and are difficult to track. For this reason the data from this survey line are not considered further. The northern part of the shoal is covered by linear and mainly ebb-directed current ripples with heights and lengths of c. 0.02 m and c. 0.1 m, respectively.

The elevation of the shoal is spatially variable (Fig. 3) and the most important characteristic is a progressive increase in its maximum

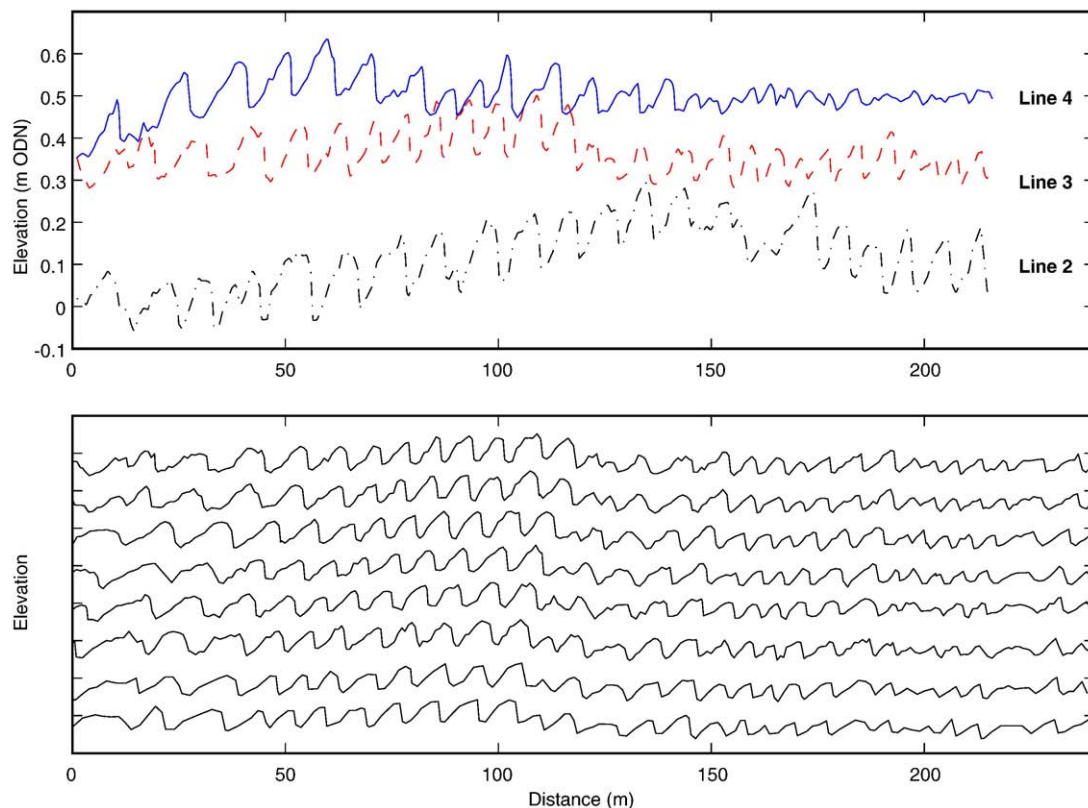


Fig. 4. Upper panel: dune morphology at the end of the survey period (12/10/07) for Lines 2–4. Lower panel: evolution of the dune morphology at Line 3 over the 3-month survey period. Successive profiles have been vertically offset by 0.2 m to ease visual comparison (chronology is from bottom to top). The x-axis runs in the up-estuary direction.

elevation in the up-estuary direction from just over 0 m ODN to just under 1 m ODN. This increase in shoal elevation is unrelated to an overall shallowing of the estuary, because the deepest part of the main channel flowing alongside the shoal remains around -1.5 m ODN. The entire shoal is dry during low tide and at its up-estuary end is only barely submerged during neap high tide.

4.2. Dune morphology, migration and sediment transport rates

An example of the spatial and temporal variability in the dune morphology for the 3-month survey period is shown in Fig. 4. The elevation of the shoal surface increases away from the tidal channel (from Line 2 to Line 4). At all three survey lines, the elevation of the shoal increases towards the centre of the survey grid ($x = 60$ – 130 m) and then decreases in the up-estuary direction. The dunes tend to be best developed over the most elevated section of the shoal. Landward of the survey lines, the dune height declines to zero and the bed becomes covered with small current ripples. Typically, the lengths and heights of well-developed dunes are 7 m and 15 cm, respectively, but considerable variability is apparent. The dunes are clearly migrating consistently in the up-estuary direction and the migration distance over the survey period was 10–20 m.

The spatial variability in dune height, migration rate and associated sediment transport for Lines 2, 3 and 4 are summarised in Fig. 5. For all three survey lines, the dunes are higher, longer and more flood-oriented at the down-estuary part of the shoal than at the up-estuary part. Together with a decrease in the dune migration rate

from 0.08 m tide⁻¹ to 0.02 m per tide⁻¹ in the up-estuary direction, this results in a concomitant reduction in the sediment transport rate. Furthermore, the dunes are largest and most dynamic closest to the main tidal channel at Line 2, and smallest and least dynamic furthest away from the main channel at Line 4. The average sediment transport over the monitored section of the shoal (Lines 2–4) over the 3-month period is 0.5 m² (per unit meter width), or 24 m³ considering each survey line represents a 16-m wide section. This equates to an annual sediment transport of 2 m² (per unit meter width) or 96 m³.

The total volume of the sediment transported over the 3-month survey period due to the migrating dunes was 0.6 – 0.9 m² at the down-estuary end of the shoal, decreasing to 0.1 – 0.4 m² at the up-estuary end. Such a 0.5 m² reduction in the amount of sediment transport rate in the up-estuary direction would result in sediment deposition over the second half of the shoal.

The temporal variability in the dune parameters and associated sediment transport rate for Lines 2, 3 and 4 are summarised in Fig. 6. A steady, albeit modest, increase in the dune height over the survey period is apparent at all survey lines, while the dune length and shape remained constant. The dune migration rate and sediment transport rate were more variable. Maximum rates occurred between Surveys 6 and 7, and minimum rates occurred between Surveys 7 and 8. Cross-referencing with Fig. 2 suggests that the main factor controlling the different transport rates between the survey periods is the number and size of the tides experienced between consecutive surveys: the spring tides between Surveys 6 and 7, and between Surveys 7 and 8, had the largest and smallest tide ranges, respectively. The average

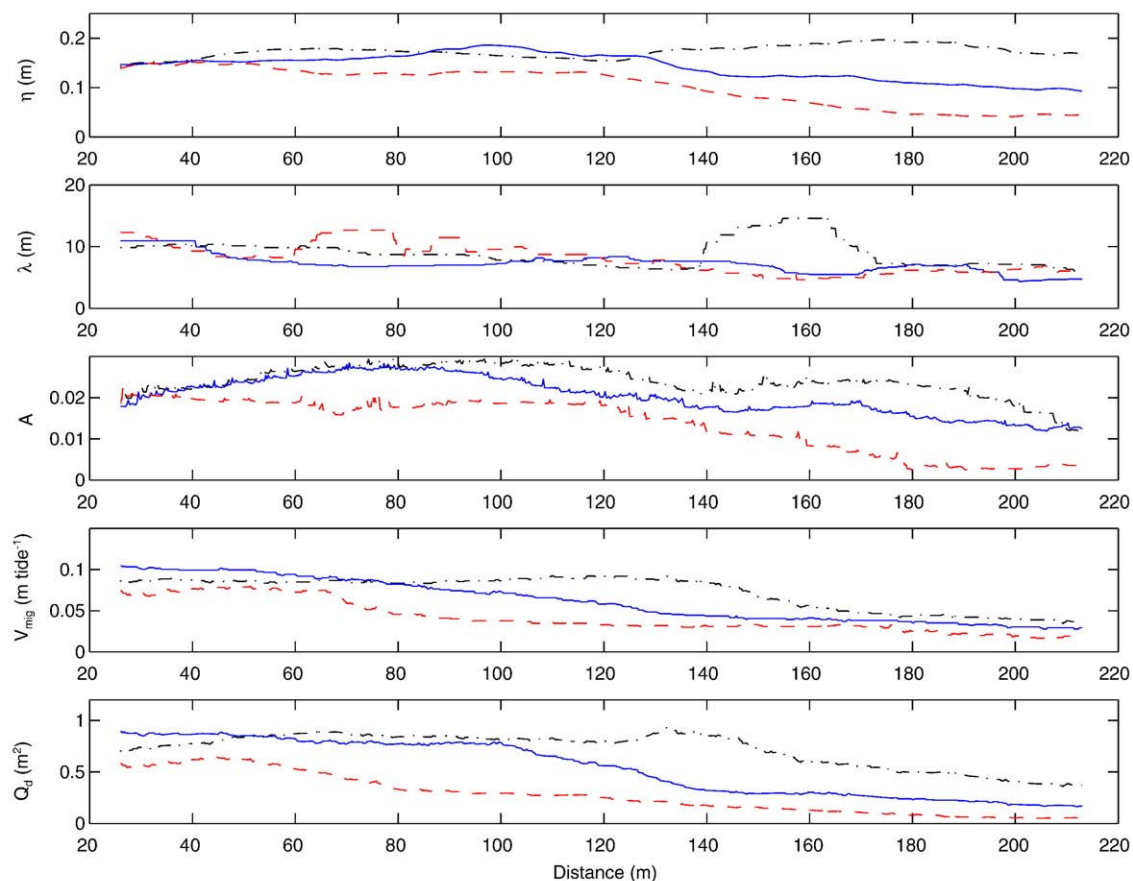


Fig. 5. Spatial variation along the length axis of the shoal in, from top to bottom: dune height η ; dune length λ ; dune shape A ; dune migration rate V_{mig} ; and total volume of sediment transported over 3-month survey period Q_d . The dune parameters η , λ , A and V_{mig} were obtained by averaging the results for the two-weekly surveys, whereas Q_d was obtained by adding the contributions of all surveys. Dash-dotted, solid and dashed lines represent survey lines 2, 3 and 4, respectively.

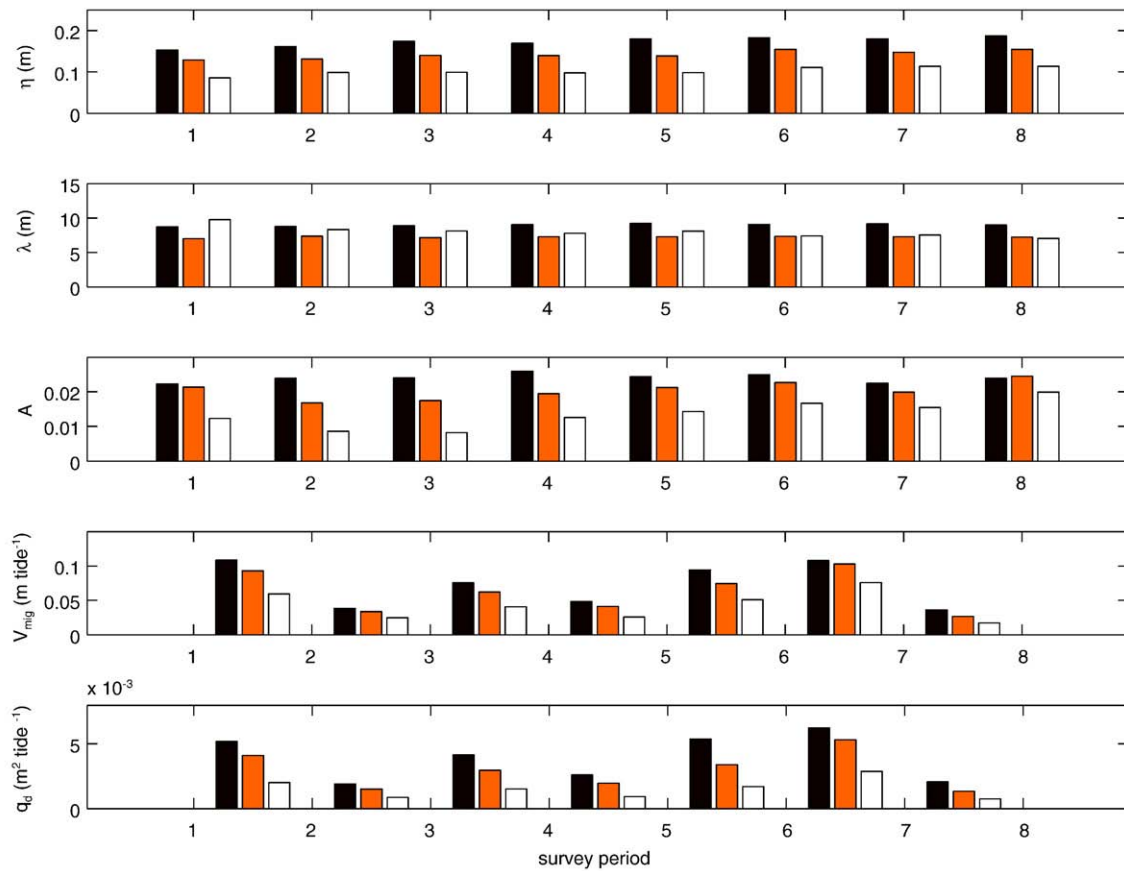


Fig. 6. Temporal variation over the 3-month survey period in, from top to bottom: dune height η ; dune length λ ; dune shape A ; dune migration rate V_{mig} ; and volumetric sediment transport rate q_d . The values were obtained by averaging the parameters over the survey lines for each of the two-weekly surveys. Black, grey and white bars represent survey lines 2, 3 and 4, respectively.

transport rate between Surveys 1 and 2 was also relatively large, because this period did not include neap tides.

Field visits during the winter months, when daily-averaged discharge often exceeds $10 \text{ m}^3 \text{ s}^{-1}$, indicate that the dune field is always present, but less pronounced than during periods of low river discharge. The results of the dune survey conducted on 10/02/08 underlines this (Table 1). There is not much difference in dune geometry between summer and winter at Line 2 (nor at Line 1; not shown), but the dunes at Line 3 in winter are somewhat smaller and less asymmetric than in summer. At Line 4, the winter dunes are very subdued and symmetric.

4.3. Current velocities, water levels and predicted sediment transport rates

Fig. 7 shows the water depth and current velocities recorded over the intertidal shoal over the 2-week measurement period, together with predicted sediment transport rates according to Eq. (4). The data span a spring-to-spring tidal cycle and a significant

variation in tide range, flow velocities and predicted sediment transport rates is apparent. High-tide water depths over the shoal are around 2 m during spring tides and around 0.5 m during neap tides. The flood-phase during spring tides lasts 3:10 h, whereas the duration of the ebb-phase is 3:40 h. Both phases have the same duration (2:50 h) during neap tides. As a result of the asymmetry in tidal duration, maximum flow velocities during springs are larger during flood ($0.4\text{--}0.5 \text{ m s}^{-1}$) than during ebb ($0.2\text{--}0.3 \text{ m s}^{-1}$). Maximum flood and ebb velocities are comparable during neaps (0.2 m s^{-1}). The tidal asymmetry in the sediment transport is even more pronounced: sand-sized sediment is only transported by flooding currents during spring tides and is therefore exclusively directed up-estuary.

The sediment transport predictions were compared with the migration of the dune recorded using stakes inserted at the base of the slip-face. No significant dune movement was observed over the neap tide period from 01/10 to 08/10, which is in direct accordance with the zero transport rates predicted for this period. Maximum migration rates (0.4 m tide^{-1}) were recorded during the first 2 tides on 28/09 and 29/09, and this also corresponds with the maximum sediment transport rate predicted for these two tides. The total migration distance of the dune over the 14-day measurement period was 2.14 m, which, using Eq. (1) and a dune height of 0.15 m, equates to a total amount of transported sediment of 0.106 m^2 . In comparison, the sediment transport predicted to have occurred over the 2-week measurement period using Eq. (4) is 0.020 m^2 . Line 3 was surveyed on 01/10 (Survey 7) and 12/10 (Survey 8) and this offers another opportunity to compare measured sediment transport rates with predictions. The total amount of sediment transported between Surveys 7 and 8 along Line 3 for $x = 80\text{--}100 \text{ m}$ (region at either side

Table 1

Comparison of dune parameters averaged over the first part of the survey grid ($x = 0\text{--}120 \text{ m}$) between summer (mean of all eight surveys during 2007) and winter (based on survey on 10/02/08) (η = dune height; λ = dune length; A = dune shape).

Survey line	Summer			Winter		
	η (m)	λ (m)	A	η (m)	λ (m)	A
Line 2	0.16	9.1	0.026	0.15	9.9	0.021
Line 3	0.16	8.0	0.024	0.11	8.7	0.010
Line 4	0.14	10.0	0.019	0.05	10.4	0.000

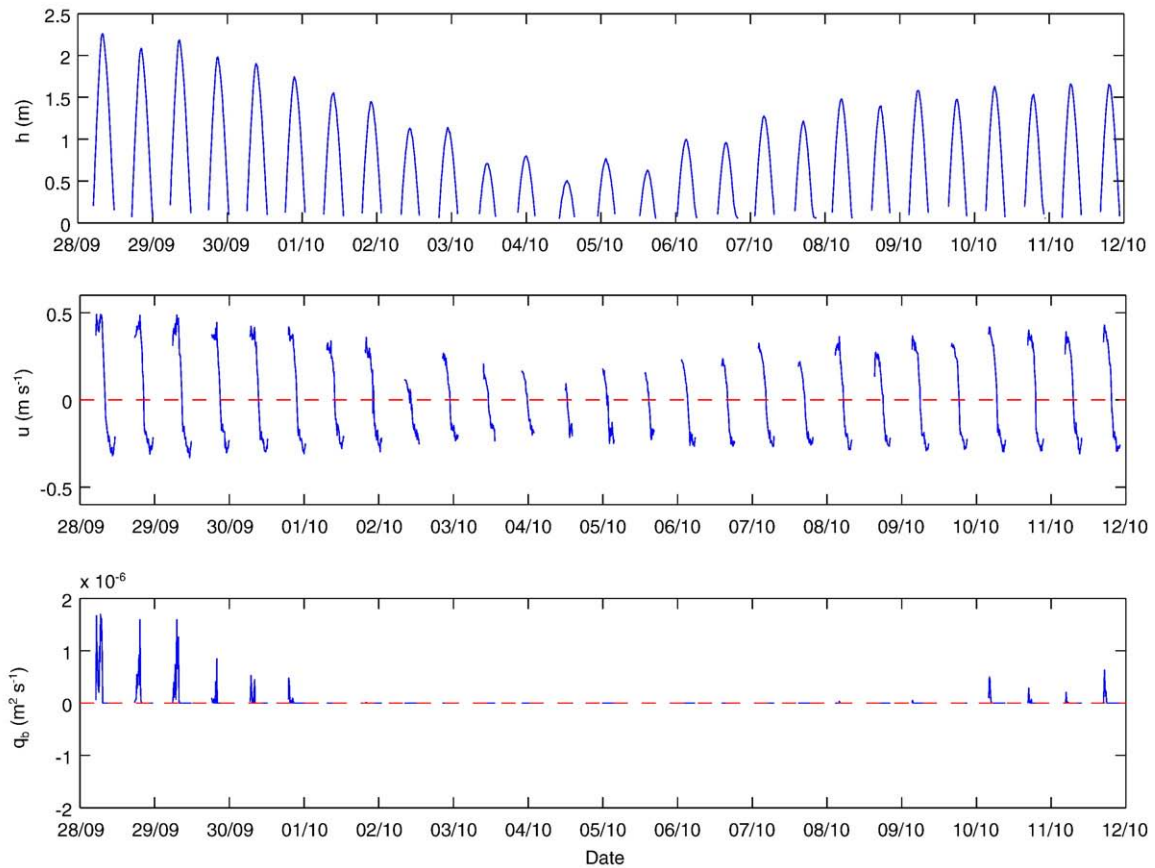


Fig. 7. Tidal hydrodynamics recorded over spring-to-spring tidal cycle at Line 3 at $x = 86$ m: water depth h (upper panel); current speed u (middle panel); and predicted bedload sediment transport rates q_b (bottom panel). Positive and negative values for u and q_b represent up-estuary (flood) and down-estuary (ebb) flows and transport rates, respectively.

of current meter location) was 0.036 m^2 . The predicted sediment transport between Surveys 7 and 8 is 0.002 m^2 .

The MPM equation thus underestimates the observed sediment transport rates by a factor 5–18. A number of factors can account for this discrepancy, but it is worth pointing out that the sediment transport predictions are rather sensitive to the sediment size d_{50} and the formulation for the bed roughness length z_0 . For example, using a d_{50} of 0.25 mm and a doubling of z_0 would reduce the ratio between observed and predicted sediment transport rates to 2–3. More importantly, due to the low flow velocities experienced during the measurement period, the model results are very sensitive to the critical Shield parameter. Using a value for θ_t of 0.05 resulted in a predicted transport of 0.020 m^2 , but using a value of 0.03 yields a transport of 0.065 m^2 , which is almost in line with the observed transport from the stake measurements (0.106 m^2). It is not the aim of this paper to come up with an improved sediment transport equation; rather, an increased understanding of the sediment dynamics on an intertidal estuarine shoal is sought. For the present purpose, therefore, the sediment transport predictions using Eq. (4) are multiplied by a factor 10 to bring the predictions in line with the measurements.

4.4. Predicting sediment transport as a function of tide range

The ‘calibrated’ transport equation (i.e., Eq. (4) with a correction factor of 10) was used to compute the volumetric sediment transport over the monitored tidal cycles, and these were correlated with the predicted tide range at Devonport to obtain a simple statistical model of sediment transport (Fig. 8). A similar approach was followed by Villard and Church (2003) who statistically related river discharge and tidal fall to sediment transport estimates in the estuary of the Fraser River, and

Whitmeyer and FitzGerald (2008) who related tide range to peak tidal current velocity in a tidal inlet. Even more comparable is the approach by Allen et al. (1994) who correlated a full year of dune migration observations, made almost every low tide, to the tidal height. The present results were fitted to a second-order polynomial to obtain an expression of transport rate per tidal cycle q_{tide} as a function of the tide range TR. The expression was obtained by conducting a least-square fit for the data with a tide range $\text{TR} \geq 3.8$ m and the resulting expression is

$$q_{\text{tide}} = 0.0028 - 0.0259(\text{TR} - 3.8) + 0.0410(\text{TR} - 3.8)^2 \quad (6)$$

with a coefficient of determination r^2 of 0.93. Eq. (6) should only be used for tide ranges (at Devonport) $\text{TR} \geq 4.3$ m; for smaller tide ranges $q_{\text{tide}} = 0$.

The measured transport estimated from dune migration at Line 3 for $x = 80$ – 100 m (location of current meter deployment) was determined over the 2-weekly survey intervals and the entire 3-month survey period. These measurements were compared with predictions from Eq. (6) using the tide range at Devonport for the experienced tidal cycles (Fig. 9). Agreement for the different survey intervals is reasonable, but, perhaps fortuitously, excellent if the entire survey period is considered: measured transport over the entire survey period was 0.76 m^2 , whereas predicted transport is 0.77 m^2 . This suggests that Eq. (6) adequately expresses the sediment transport rate as a function of the tide range. It is also noted that the sediment transport over the survey period measured at the instrument location (0.76 m^2) is about 50% larger than grid average (0.51 m^2); therefore, Eq. (6) is fairly representative of the area of the shoal covered by the survey grid.

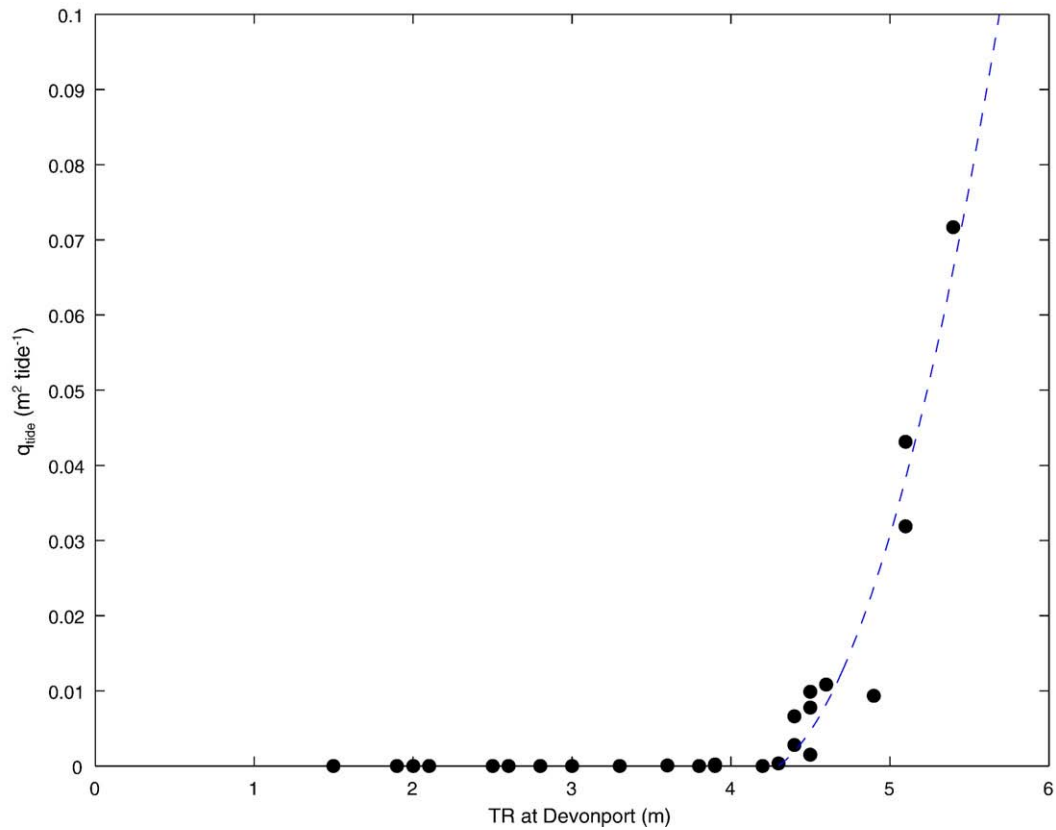


Fig. 8. Scatter plot of the predicted volumetric sediment transport rate per tide q_{tide} and the tide range TR at Devonport with the least-squares fit.

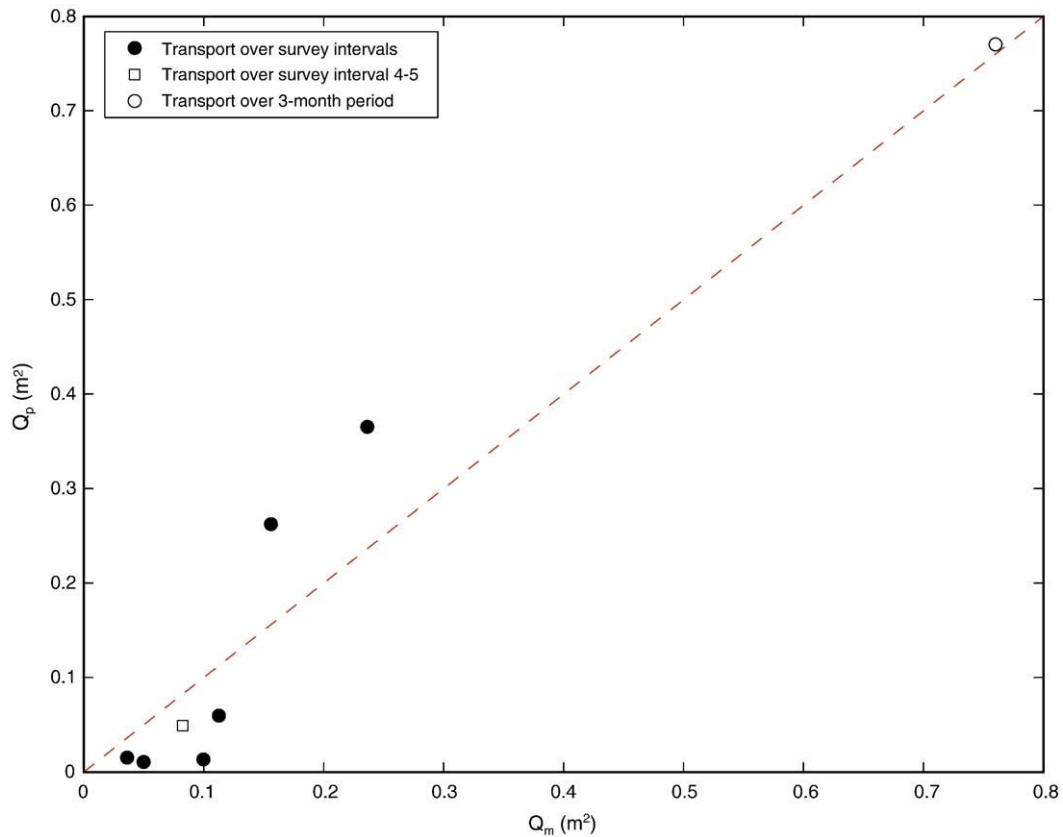


Fig. 9. Comparison between measured sediment transport Q_m over the 2-weekly survey intervals and the transport Q_p predicted using Eq. (6) and the tide range at Devonport. The dashed line represents exact agreement. The transport for survey interval 4–5 has been represented by a different symbol because this period was characterised by relatively high river discharge.

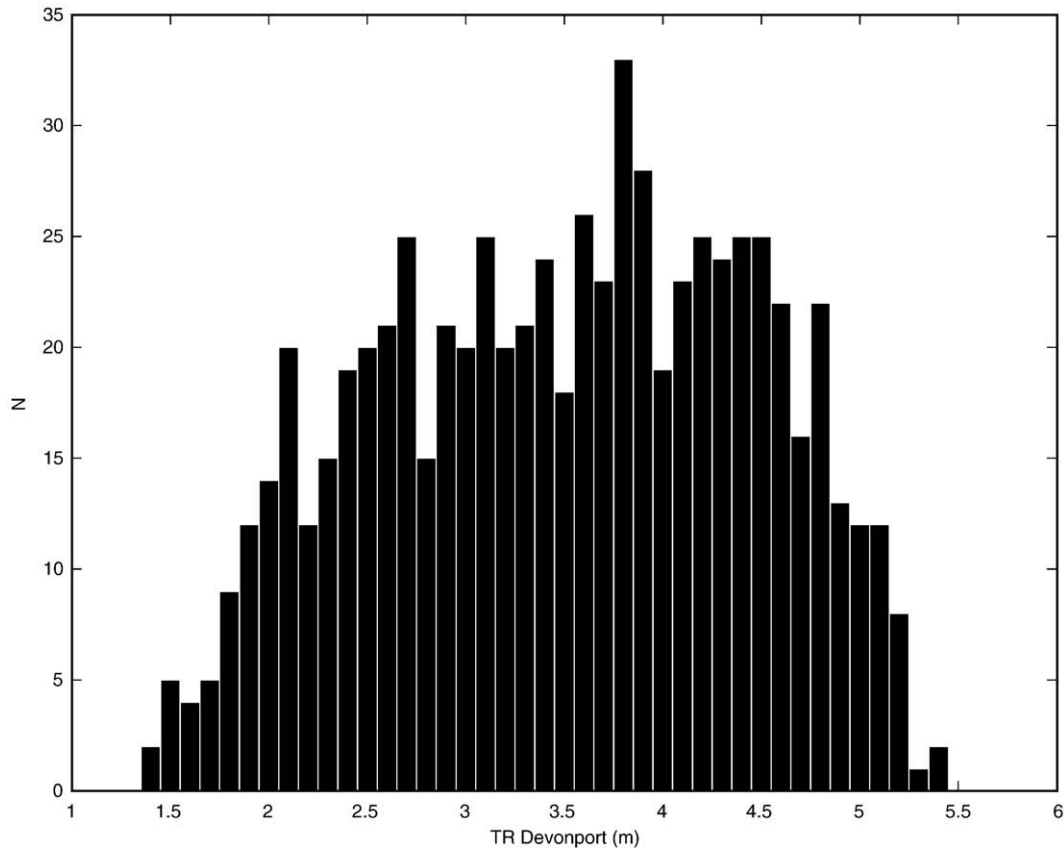


Fig. 10. Absolute frequency distribution of the tide range TR at Devonport for 1 year of data (13/07/2007–12/07/2008). N represents the number of tides.

4.5. Estimating net annual sediment transport

One year of tidal predictions was obtained for Devonport (Fig. 10) and these data were used to estimate the annual sediment transport across the intertidal shoal by summing the sediment transport contributions of all tidal cycles computed using Eq. (6). The annual transport was 2.6 m^2 and was accomplished by 26% of the tides (only those with a tide range $\text{TR} \geq 4.3 \text{ m}$). More than half (53%) of the annual transport was generated by tides with a tide range $\text{TR} \geq 5 \text{ m}$. Such tides only occur for 5% of the time (35 tides per year), emphasising the importance of the extreme tides in driving sediment transport processes on the intertidal shoal (cf. Allen et al., 1994). It was argued in Section 4.4 that Eq. (6) can be considered fairly representative of intertidal shoal area covered by the survey grid. This is further supported by the close agreement between the predicted annual transport (2.6 m^2) and measured transport averaged over the survey grid extrapolated over a year (2.0 m^2).

5. Discussion

The dunes at Aunemouth Sands are characterised by heights η of $0.05\text{--}0.2 \text{ m}$ and lengths λ of $5\text{--}10 \text{ m}$. Their steepness η/λ is c. 0.015 and they are highly two-dimensional with crest lengths generally exceeding 50 m . Two-dimensional dunes develop in fine-to-medium sand when mean flow velocities exceed 0.5 m s^{-1} (Ashley, 1990) and for the dunes to become three-dimensional current velocities in excess of 0.7 m s^{-1} are required (Terwindt and Brouwer, 1986; Larcombe and Ridd, 1995; Larcombe and Jago, 1996). The peak flows during spring tides, which control the dune dynamics, stay within these narrow boundaries; therefore, the dunes remain two-dimensional throughout the neap-spring tidal cycles. They are largely moribund during neap tides.

It is of interest to compare the dune geometry with that predicted according to equilibrium dune models. The model of Allen (1968), which only requires flow depth h , is used here as a basis for comparison

$$\eta = 0.086h^{1.19} \quad (7)$$

$$\lambda = 1.16h^{1.55} \quad (8)$$

The dunes are only active under spring high tide conditions, when $h = 1\text{--}2 \text{ m}$, and for such depth range Eqs. (7) and (8) predict $\eta = 0.09\text{--}0.2 \text{ m}$ and $\lambda = 1.2\text{--}3.4 \text{ m}$, respectively. According to Ashley (1990) the dune height is related to the dune length according to

$$\eta = 0.0677\lambda^{0.8098} \quad (9)$$

For the observed dune lengths of 5 and 10 m , Eq. (9) predicts dune heights of 0.25 and 0.44 m , respectively. The model predictions are clearly at odds with the observations and the most parsimonious conclusion is that the dune heights are predicted well, but that the dune lengths are significantly under-predicted.

It is unusual for disequilibrium dunes to have larger wave lengths than expected; one would expect developing dunes to be either too low and/or too short (Kostaschuk and Best, 2005). For fluvial dunes, the occurrence of low steepness dunes is generally ascribed to the importance of suspended sediment transport (Best, 2005). Application of the sediment transport model of van Rijn (1993; Eqs. (A3)–(A7)) showed that the majority of the sediment transport may have occurred as suspended load; however, a dominance of suspended load would result in a flattening of the dunes, not a lengthening. Eqs. (7)–(9) are mainly based on subaqueous dune data collected from flumes or riverine environments under uni-directional flow conditions, whereas intertidal dunes experience reversing currents over a tidal

cycle. In addition, the flow field associated with intertidal dunes is characterised by a distinct neap-spring modulation. In this context, the investigations of Larcombe and Jago (1996) and Carling et al. (2006) are of interest. In both studies, the observed intertidal dune dimensions conformed reasonably well to Eq. (9) during spring tides, but the dunes were either too long (Larcombe and Jago, 1996) or too small (Carling et al., 2006) during neap tides. It should also be noted that the scaling of dunes with the flow depth has been challenged; for example, Bartholdy et al. (2005) convincingly demonstrated the important control of sediment size on dune length. Clearly, more observational data are required to address the notion of equilibrium dune geometry in intertidal settings.

Average and maximum dune migration rates reported here are 0.05–0.1 and 0.4 m tide⁻¹, respectively, and are significantly less than reported elsewhere in the literature from intertidal settings (e.g. Larcombe and Ridd, 1995; Larcombe and Jago, 1996; Allen et al., 1994; Hoekstra et al., 2004; Carling et al., 2006). This is mainly attributed to the modest current velocities. The field observations show that, the maximum flood velocities (0.5 m s⁻¹) are above the threshold for dune migration (the dunes migrate), whereas the maximum ebb velocities (0.35 m s⁻¹) are below the threshold (no evidence of any of the dunes changing their orientation, or even developing an ebb-directed cap). Larcombe and Jago (1996) found a dune migration threshold of 0.53–0.57 m s⁻¹ in 0.28-mm sand, whereas Larcombe and Ridd (1995) observed a dune migration threshold of 0.5–0.6 m s⁻¹ in 0.45-mm sand. Allen et al. (1994) found a dune migration threshold of 0.65 m s⁻¹ for a sediment size of 0.2–0.25 mm. Another contributing factor to the low migration rates is the short duration that the dunes are exposed to tidal currents. Tidal duration also explains the difference in migration rates across the shoal, with the largest (smallest) rates found at the survey line with the lowest (highest) elevation (refer to Fig. 4).

Previously reported dune migration threshold velocities are, however, mean flow velocities, whereas in the present study velocities were recorded 0.25 m from the bed. Given the steep velocity gradient characteristic of flows over dunes (e.g., Kostaschuk and Villard, 1996; Kostaschuk et al., 2004), our measured near-bed flow velocities are expected to be significantly less than the depth-averaged velocity. Using Eqs. (2) and (3) and a threshold Shields parameter of $\theta_t = 0.05$ results in sediment threshold flow velocities of 0.38, 0.40 and 0.43 m s⁻¹ for water depths of 0.5, 1, and 2 m, respectively. Using the equations of van Rijn (1993; Eq. (A3)), the sediment threshold velocities are somewhat lower at 0.31, 0.33 and 0.36 m s⁻¹ for water depths of 0.5, 1, and 2 m, respectively. The implication is that the maximum flood flow velocities are greater than the threshold of motion by about a factor of 1.5, whereas the ebb velocities are just below the threshold of motion.

The agreement between the observed threshold velocity for dune migration (between 0.35 and 0.5 m s⁻¹) and the predicted threshold velocity (c. 0.4 m s⁻¹) suggests that the parameterisation of the bed shear stress using $z_0 = d_{50}/12$ is appropriate. This still leaves the under-prediction of the measured sediment transport rates using the MPM equation by a factor 10 unexplained. Bedload transport rates were also predicted using the equations of Madsen (1991; Eq. (A1)), Nielsen (1992; Eq. (A2)) and van Rijn (1993; Eqs. (A3)–(A7)). The results listed in Table 2 show that although these equations do a slightly better job, the observed sediment transport rates remain under-predicted by at least a factor 2. The poor performance of the models is mainly explained by the modest flow velocities, even during spring tides, because bedload predictors tend to underestimate transport rates under low flow conditions (van den Berg, 1987). In fact, only a modest reduction of the critical Shields parameter from 0.05 to 0.03 was shown to result in reasonably agreement between predicted and observed sediment transport. Model performance is worst when only the period 01/10–12/10 is considered and during this time the flows were weakest (refer to Fig. 7). Additionally, all

Table 2

Comparison between observed sediment transport recorded over the 2-week period of flow measurements based on dune migration and the models of Meyer-Peter and Muller (1948), Madsen (1991), Nielsen (1992) and van Rijn (1993).

Measurement period	Dune migration	Meyer-Peter and Muller (1948)	Madsen (1991)	Nielsen (1992)	van Rijn (1993)	
					Bedload	Suspended load
28/09–12/10	0.106	0.020	0.023	0.052	0.010	0.035
01/10–12/10	0.036	0.002	0.003	0.007	0.002	0.006

The units are m³ per unit m width (m²).

equations are bedload predictors and, considering the grain size of the dune sediment, it is possible that a significant proportion of sediment transport may have occurred by suspension. Application of the sediment transport model of van Rijn (1993) indicates a ratio between suspended load transport and bedload transport of 3.5. Deposition of the suspended load in the troughs behind the dunes contributes to the lee-side accumulation (Kostaschuk and Best, 2005) and, hence, dune migration not accounted for in the bedload predictors.

Because the dunes on Aunemouth Sands only migrate during the flood phase of the tide, it is relatively straightforward to derive net sediment transport rates due to the migrating dunes into the estuary. The annual flood-driven and up-estuary sediment transport for a section of Aunemouth Sands comprising an area of 48 × 240 m (Lines 2–4) was estimated at 2.0 m² based on measurements and 2.6 m² based on model predictions. This equates to a total sediment transport across the width of the survey grid of $O(100 \text{ m}^3)$. Close agreement between measurements and predictions provides strong support for the approach adopted in this study. Of most significance to shoal development is the fate of this sediment, or, to be more specific, the gradient in the sediment transport along the transport path. A reduction of the total volume of the sediment transported over the 3-month survey period of 0.5 m² was recorded from the down-estuary end of the dune field to the up-estuary end. Because gradients in the sediment transport are responsible for morphological change, they can be used to estimate the long-term development of the intertidal shoal. Extrapolating the dune migration results to one year (12 months) implies an overall up-estuary reduction in the transport rate of 2 m² year⁻¹. Assuming that this reduction occurs over the entire 240-m long survey grid and further considering a sediment porosity of 0.4, the estimated amount of accretion per year that would occur is 0.005 m year⁻¹ or 0.5 cm year⁻¹ ($(1-0.4) \times 2 \text{ m}^2 \text{ year}^{-1} / 240 \text{ m}$). Accretion rates up-estuary from the dune field, where only small current ripples are present, would be significantly less.

The likely source of the sediment transported on the shoal is the down-estuary margin of the intertidal shoal, located seaward of the survey grid. The tidal channel may also be a contributor of sediment, but even during spring tides the flood velocities rarely exceed 0.4 m s⁻¹ (Uncles et al., 2007) and the flood current thus accelerates as it leaves the tidal channel and ‘spills’ onto the shoal. The morphological development of the shoal is thus akin the migration of a large bedform, characterised by upstream (up-estuary) erosion and down-stream (down-estuary) accretion. The morphological change is very slow and requires accurate morphological surveys on a decadal time scale to demonstrate convincingly. Nevertheless, flood-directed dunes are always present on Aunemouth Sands and their presence and dynamics are clear evidence of consistent flood-directed sediment transport. The rate of accretion $O(0.5 \text{ cm year}^{-1})$ also supports the opinion of local residents who have observed a significant shallowing of the shoal over the last few decades.

The 3-month dune survey was conducted over a period of relatively low river discharge. Previous studies have indicated that river discharge can have a significant effect on dune dynamics in estuarine settings (Bryce et al., 1998; Weihua et al., 2008) and it may be questioned whether the present results obtained over a low

discharge period are representative for the whole year. Three observations support this assumption. Firstly, the period with the largest river discharge (from Surveys 4 to 5), with daily-averaged river discharge in excess of $5 \text{ m}^3 \text{ s}^{-1}$, did not reveal significantly less sediment transport compared to intervals with similar tide ranges, but with a smaller river discharge (Fig. 9). Secondly, tidal flow measurements conducted by Uncles et al. (2007) in the tidal channel at Bantham Harbour did not indicate a significant difference in flood and ebb velocities between summer (freshwater discharge $1\text{--}2 \text{ m}^3 \text{ s}^{-1}$) and winter (freshwater discharge $2\text{--}14 \text{ m}^3 \text{ s}^{-1}$). Thirdly, field visits during the winter months and the survey conducted on 10/02/2008 show that even under conditions of large freshwater discharge the dunes remain directed up-estuary. The effect of river discharge on the dynamics of the dune field is limited, although not insignificant (see Table 2), because the tidal prism is very large relative to the discharge from the river. Using the tidal prism estimates obtained from the 1-line tidal model of Uncles et al. (2007), the average spring tidal discharge at Bantham Harbour is $67 \text{ m}^3 \text{ s}^{-1}$ during a 5-h flooding tide and $48 \text{ m}^3 \text{ s}^{-1}$ during a 7-h ebbing tide, which is 7–10 times greater than the monthly mean winter river discharge of $7 \text{ m}^3 \text{ s}^{-1}$ (Uncles et al., 2007). Furthermore, due to the high elevation of the intertidal shoal, flows only affect the shoal close to high tide, when the channel cross-sectional area is maximum and the effect of river discharge should be minimum.

Allen et al. (1994) found in their study conducted at Wells-next-the-Sea on the east coast of England that positive storm surges contributed as much to dune migration than astronomical tides. The effect of storm surges on the dune dynamics on Aunemouth Sands is expected to be limited. The 1:50 year storm surge height for the south coast of Devon is c. 0.5 m, compared to 2 m for the east coast of England (Lowe and Gregory, 2005). In addition, the dune field on Aunemouth Sands is located in a very sheltered location, whereas the dunes studied by Allen et al. (1994) are situated in the mouth of a funnel-shaped estuary.

Estuarine infill processes occur over long time scales (decades to millennia) and geological research methods involving dating techniques are required to quantify accretion rates. However, this investigation demonstrates that accurate and well-designed process measurements of dune dynamics and tidal currents can provide useful information on the longer term evolution of estuarine intertidal shoals. This was achieved by formulating an empirical relation between the tide range and onshore sediment transport on the intertidal shoal (using flow measurement and a bed load equation), and taking into account the sediment transport gradient along the shoal (derived from dune surveys). The resulting equation is, of course, highly site-specific (cf. Allen et al., 1994), and only represents the sediment transport associated with migrating dunes, but can be determined with relative ease at other sandy, shallow (flood-dominant) estuaries using a similar methodology. In fact, if dune migration rates and associated sediment fluxes are recorded every low tide over a sufficiently long period (at least two weeks to cover half a lunar tidal cycle), then the empirical equation relating tide range to dune sediment transport can be derived without having to consider flow measurements.

6. Conclusions

The subaqueous dunes on the intertidal shoal of Aunemouth Sands are characterised by heights and lengths of 0.05–0.2 m and 5–10 m. Compared to equilibrium models of dune dimensions based on the water depth (Allen, 1968; Ashley, 1990), the dune height is predicted well, but the dune length is under-predicted. Repeat morphological surveys reveal that the dunes migrate mainly during spring tides and a total migration distance of 10–20 m over the 3-month period was obtained. Dune migration was solely in the up-estuary direction, because the sediment transport processes on the shoal are controlled

by a distinct tidal asymmetry with maximum flow velocities during flood ($0.4\text{--}0.5 \text{ m s}^{-1}$) significantly stronger than during ebb ($0.2\text{--}0.3 \text{ m s}^{-1}$). In fact, even the strongest ebb flows barely exceed the threshold of sediment motion. The rates of dune migration are significantly less than reported elsewhere in the literature from intertidal settings. This is ascribed to the modest flow velocities encountered and the relatively high elevation of the dunes in the tidal frame limiting their tidal exposure to only a few hours each tide.

Comparison between measured volumetric sediment transport rates (derived from dune dimensions and migration rates) and bedload equations shows that theory significantly under-predicts the observations. The poor performance of the bedload predictors is attributed to the modest flow velocities encountered (bedload predictors do not perform well near the threshold of motion) and, possibly, the importance of suspended load transport. Application of the 'simplified' sediment transport model of van Rijn (1993) indicates a ratio between suspended load transport and bedload transport of 3.5, and the deposition of suspended load in the troughs behind the dunes contributes to dune migration that is not accounted for in the bedload predictors.

The Meyer-Peter and Muller (1948) equation was empirically calibrated to obtain an expression for the flood-driven sediment transport rate as a function of tide range. Using one year of tidal predictions, an annual volumetric sediment transport of 2.6 m^3 per unit meter width was predicted across a 48-m wide section of shoal. This estimate compares favourably with the annual volumetric sediment transport based on dune measurements (2.0 m^3). Using the notion that the transport rate due to dune migration decreases along the intertidal shoal in the up-estuary direction to zero at its up-estuary end, a vertical accretion of 0.5 cm yr^{-1} was predicted.

The main implication of our study is that accurate and well-designed process measurements of dune dynamics and tidal currents can provide useful information on the longer term evolution of intertidal shoals in sandy, shallow (flood-dominant) estuaries.

Acknowledgements

We would like to thank the Aune Conservation Association for their ongoing support for University of Plymouth research in the Avon estuary. Jamie Quinn of the Cartographic Research Unit of the School of Geography, University of Plymouth produced Fig. 1. Thanks also to Reg Uncles for running his 1-line tidal model and providing the tidal prism estimates.

Appendix A

The equations of Madsen (1991) and Nielsen (1992) are very similar to the MPM equation in that all formula predict the dimensionless sediment transport Φ (Eq. (4)) as a function of the (skin friction) Shields parameter θ (Eq. (3)), taking into account the value of θ at the threshold of motion ($\theta_t = 0.05$).

The Madsen (1991) equation states

$$\Phi = F_M (\theta^{0.5} - 0.7\theta_t^{0.5}) (\theta - \theta_t) \quad (\text{A1})$$

where F_M is $8/\tan\phi$ (angle of repose $\phi = 33^\circ$), and the Nielsen (1992) equation states

$$\Phi = 12\theta(\theta - \theta_t)^{0.5} \quad (\text{A2})$$

The 'simplified' sediment transport model of van Rijn (1993) uses the mean flow velocity and does not require consideration of the

water surface slope or shear stress measurements, and the relevant equations are

$$q_b = 0.005uh \left[\frac{u - u_t}{[(s-1)gd_{50}]^{0.5}} \right]^{2.4} \left(\frac{d_{50}}{h} \right)^{1.2} \quad (A3)$$

$$q_s = 0.012uh \left[\frac{u - u_t}{[(s-1)gd_{50}]^{0.5}} \right]^{2.4} \left(\frac{d_{50}}{h} \right) D_*^{-0.6} \quad (A4)$$

$$u_t = 0.19d_{50}^{0.1} \log \left(\frac{4h}{d_{90}} \right) \quad \text{for } 0.1 \leq d_{50} \leq 0.5 \text{ mm} \quad (A5)$$

$$u_t = 8.5d_{50}^{0.6} \log \left(\frac{4h}{d_{90}} \right) \quad \text{for } 0.5 < d_{50} \leq 2 \text{ mm} \quad (A6)$$

$$D_* = d_{50} \left[\frac{g(s-1)}{\nu^2} \right]^{1/3} \quad (A7)$$

where q_b and q_s are volumetric bedload and suspended load sediment transport rate per unit width ($\text{m}^2 \text{s}^{-1}$), u is depth-averaged flow velocity, h is flow depth, u_t is sediment threshold velocity, s is ratio of densities of sediment and water ($s = 2.58$), g is gravity ($g = 9.8 \text{ m s}^{-2}$), d_{50} is median bed sediment size ($d_{50} = 0.3 \text{ mm}$), d_{90} is the coarsest ninetieth percentile of bed sediment size ($d_{90} = 0.45 \text{ mm}$) and ν is kinematic viscosity ($\nu = 1 \times 10^{-6} \text{ m}^2 \text{ s}^{-1}$).

References

- Admiralty Tide Tables, 2007. United Kingdom and Ireland (including European Channel Ports). Hydrographic Office, Taunton, UK.
- Allen, J.R.L., 1968. The nature and origin of bedform hierarchies. *Sedimentology* 10, 161–172.
- Allen, J.R.L., Friend, P.F., Lloyd, A., Wells, H., 1994. Morphodynamics of intertidal dunes – a year-long study at Lifeboat-Station-Bank, Wells-next-the-Sea, eastern England. *Philos. Trans. R. Soc. Lond. Ser. A: Math. Phys. Sci.* 347, 291–345.
- Ashley, G.M., 1990. Classification of large-scale subaqueous bedforms: a new look at an old problem. *J. Sediment. Petrol.* 60, 160–172.
- Austin, M.J., Masselink, G., O'Hare, T.J., Russell, P.E., 2007. Relaxation time effects of wave ripples on tidal beaches. *Geophys. Res. Lett.* 34, L16606.
- Bartholdy, J., Flemming, B.W., Bartholoma, A., Ernsten, V.B., 2005. Flow and grain size control of depth-dependent simple subaqueous dunes. *J. Geophys. Res. Earth Surf.* 110, F04S16.
- Bates, C.R., Oakley, D.J., 2004. Bathymetric sidescan investigation of sedimentary features in the Tay estuary, Scotland. *Int. J. Remote Sens.* 25, 5089–5104.
- Best, J., 2005. The fluid dynamics of river dunes: a review and some future research directions. *J. Geophys. Res. Earth Surf.* 110, F04S02.
- Bryce, S., Larcombe, P., Ridd, P.V., 1998. The relative importance of landward-directed tidal sediment transport versus freshwater flood events in the Normanby River estuary, Cape York Peninsula, Australia. *Mar. Geol.* 149, 55–78.
- Carling, P.A., Radecki-Pawlik, A., Williams, J.J., Rumble, B., Meshkova, L., Bell, P., Breakspear, R., 2006. The morphodynamics and internal structure of intertidal fine-gravel dunes: Hills flats, Severn estuary, UK. *Sediment. Geol.* 183, 159–179.
- Cheng, H.Q., Kostaschuk, R., Shi, Z., 2004. Tidal currents, bed sediments, and bedforms at the South Branch and the South Channel of the Changjiang (Yangtze) estuary: implications for the ripple–dune transition. *Estuaries* 27, 861–866.
- Cointre, L., (2008) The estuarine dynamics of the Avon Estuary, Devon. Unpublished MSc thesis, Applied Marine Science, University of Plymouth.
- Dalrymple, R.W., Zaitlin, B.A., Boyd, R., 1992. Estuarine facies models: conceptual basis and stratigraphic implications. *J. Sediment. Petrol.* 62, 1130–1146.
- Davidson, N.C., 1991. Nature Conservation and Estuaries in Great Britain. Nature Conservancy Council, Peterborough.
- Draper, L., 1991. Wave climate atlas of the British Isles. Offshore Technology Report, Department of Energy, OTH 89 303. HMSO, London.
- Francken, F., Wartel, S., Parker, R., Taverniers, E., 2004. Factors influencing subaqueous dunes in the Scheldt Estuary. *Geo Mar. Lett.* 24, 14–21.
- Friedrichs, C.T., Aubrey, D.G., 1988. Non-linear tidal distortion in shallow well-mixed estuaries: a synthesis. *Estuar. Coast. Shelf Sci.* 27, 521–545.
- Friedrichs, C.T., Hamrick, J.M., 1996. Effects of channel geometry on cross sectional variations in along channel velocity in partially stratified estuaries. *Coast. Estuar. Stud.* 53, 283–300.
- Gonzalez, R., Eberli, G.P., 1997. Sediment transport and bedforms in a carbonate tidal inlet; Lee Stocking Island, Exumas, Bahamas. *Sedimentology* 44, 1015–1030.
- Hoefel, F., Elgar, S., 2003. Wave-induced sediment transport and sand bar migration. *Science* 299, 1885–1887.
- Hoekstra, P., Bell, P., van Santen, P., Roode, N., Levoy, F., Whitehouse, R., 2004. Bedform migration and bedload transport on an intertidal shoal. *Cont. Shelf Res.* 24, 1249–1269.
- Kostaschuk, R., Villard, P., 1996. Flow and sediment transport over large subaqueous dunes: Fraser River, Canada. *Sedimentology* 43, 849–863.
- Kostaschuk, R., Villard, P., Best, J., 2004. Measuring velocity and shear stress over dunes with acoustic Doppler profiler. *J. Hydraul. Eng.* 130, 932–936.
- Kostaschuk, R., Best, J., 2005. Response of sand dunes to variations in tidal flow: Fraser Estuary, Canada. *J. Geophys. Res. Earth Surf.* 110, F04S04.
- Larcombe, P., Ridd, P.V., 1995. Megaripple dynamics and sediment transport in a mesotidal mangrove creek: implications for palaeoflow reconstruction. *Sedimentology* 42, 593–606.
- Larcombe, P., Jago, C.F., 1996. The morphological dynamics of intertidal megaripples in the Mawddach Estuary, North Wales, and the implications for palaeoflow reconstructions. *Sedimentology* 43, 541–559.
- Lowe, J.A., Gregory, J.M., 2005. The effects of climate change on storm surges around the United Kingdom. *Philos. Trans. R. Soc. Lond.* 363, 1313–1328.
- Madsen, O.S., 1991. Mechanics of cohesionless sediment transport in coastal waters. *Proceedings Coastal Sediments '91*. ASCE, New York, pp. 15–27.
- Meyer-Peter, E., Muller, R., 1948. Formulas for bedload transport. *Proceedings 2nd meeting of the International Association for Hydraulic Research, Stockholm*, pp. 39–64.
- Millin, S., (2006) The application of GIS to illustrate the effects of geomorphological changes on the Avon estuary in south Devon. Unpublished BSc thesis, Geography, University of Plymouth.
- Nielsen, P., 1992. Coastal bottom boundary layers and sediment transport. *Advanced Series on Ocean Engineering*, vol. 4. World Scientific Publishing, Singapore.
- Shepard, S.A., Hails, J.R., 1984. The dynamics of a megaripple field in northern Spencer Gulf, South Australia. *Mar. Geol.* 61, 249–263.
- Soulsby, R.L., 1997. *Dynamics of Marine Sands*. Thomas Telford, London.
- Terwindt, J.H.J., Brouwer, M.J.N., 1986. The behaviour of intertidal sand waves during neap-spring tide cycles and the relevance for palaeoflow reconstructions. *Sedimentology* 33, 1–31.
- Uncles, R.J., Stephens, J.A. and Harris, C., (2007) Final report on the sediments and hydrography of the Devonshire Avon estuary. Unpublished Report, Plymouth Marine Laboratory, Plymouth.
- van den Berg, J.H., 1987. Bedform migration and bed-load transport in some rivers and tidal environments. *Sedimentology* 34, 681–698.
- van Rijn, L.C., 1993. *Principles of Sediment Transport in Rivers, Estuaries and Coastal Seas*. Aqua, Amsterdam.
- Villard, P.V., Church, M., 2003. Dunes and associated sand transport in a tidally influenced sand-bed channel: Fraser River, British Columbia. *Can. J. Earth Sci.* 40, 115–130.
- Villard, P.V., Church, M., 2005. Bar and dune development during a freshet: Fraser River Estuary, British Columbia, Canada. *Sedimentology* 52, 737–756.
- Weihua, L., Cheng, H.-E., Jiufa, L., Ping, D., 2008. Temporal and spatial changes of dunes in the Changjiang (Yangtze) estuary, China. *Estuar. Coast. Shelf Sci.* 77, 169–174.
- Whitmeyer, S.J., FitzGerald, D.M., 2008. Episodic dynamics of a sand wave field. *Mar. Geol.* 252, 24–37.
- Williams, J.J., Carling, P.A., Bell, P.S., 2006. Dynamics of intertidal gravel dunes. *J. Geophys. Res. Oceans* 111, C06035.